NUMERICAL COMPUTATION OF TRANSIENT AND STEADY-STATE PERIODIC THERMAL WAVE DISTRIBUTION IN HOMOGENEOUS MEDIA

P.M.Patel, S.K. Lau and D.P. Almond

School of Materials Science
University of Bath
Bath, Avon, England, BA2 7AY

INTRODUCTION

Thermal wave inspection techniques utilise controlled heat diffusion to probe the surface and subsurface structure of a component [1-3]. Various techniques have been developed which use localised intensity or spatially modulated laser heating for thermal wave generation [2] and a variety sensors, acoustic, optical, and thermal, for their detection [3,4]. The quantitative application of these techniques rely on the computation of the surface temperature and its relation to the internal or surface thermal structure. Analytical solutions for the surface temperature are available for the inspection of layered structures, for example, a coating on a substrate. For samples containing defects of a finite geometry (spherical, lens, cylindrical, disc void/inclusion etc) analytical solutions are difficult to obtain. In these cases numerical methods are employed to solve the heat diffusion equation for the surface temperature. In this paper we discuss the application and limitations of finite difference method for periodic and transient heat diffusion.

NUMERICAL SOLUTIONS

Finite difference, finite element, and boundary element techniques are three very general numerical methods currently utilised in solving partial differential equations [5-7]. The finite difference method of obtaining a solution of a given partial differential equation is to approximate the derivatives appearing in the equation, by a set of values of the function at a selected number of points called nodes. The most popular way to generate these approximations is through the use of Talyor series [5]. In the finite element method, the sample is divided into "elements" over the entire domain. Suitable functions are then approximated over the elements which satisfy the boundary conditions. With the boundary element method the sample divided into "elements" along sample boundaries (or points of interest). They also make use of the fundamental solutions for the computation of temperature and flux distribution. Further details of these methods can be found in [6,7].

Although all the above methods can be used for calculating the temperature distribution each method has its pro and cons. For simple geometry samples the finite difference method is most suitable in terms of efficiency and ease of calculation. The finite element method is ideally suited to samples of complex boundaries, and the boundary element method are preferable over finite elements techniques when computing the temperature field in "infinite" samples [7].

Review of Progress in Quantitative Nondestructive Evaluation, Vol. 9
Edited by D.O. Thompson and D.E. Chimenti
Plenum Press, New York, 1990

PERIODIC TEMPERATURE DISTRIBUTIONS

Consider first heat diffusion in one dimension. Assume that the sample has uniform thermal properties and its surface is periodically heated. The heat diffusion equation can then be written as:

$$k\frac{d^2T}{dx^2}-\rho C\frac{dT}{dt}=\begin{cases}-Q.e^{j\omega t} & \textit{at the surface}\\ 0 & \textit{in the solid}\end{cases} \tag{1}$$

where T is the temperature and x the spatial coordinate. k, C and ρ are respectively the sample thermal conductivity, specific heat capacity and sample density. Q is the applied periodic surface heat flux. After the initial surface transient the sample temperature can be assumed to be periodic. The substitution $T(x)=T(x).e^{j\omega t}$ can be made in equation 1 to eliminate the time derivative. The finite difference method then proceeds as follows [8]. First divide the sample into N nodal points, then apply the energy balance method at each nodal point to obtain the finite difference nodal equations. For example at the node i, the sum of the energy flux entering and leaving the node is zero:

$$\frac{k(T_{i-1}-T_i)}{\Delta x}+\frac{k(T_{i+1}-T_i)}{\Delta x}-j\omega\rho C\Delta x=0 \tag{2}$$

where Δx is the nodal spacing. Similar difference equations can be written down for the surface and rear face nodes

$$-AT_1+T_2=\frac{-Q\Delta x}{k} \tag{3}$$

$$T_{N-1}-AT_N=0 \qquad \textit{where} \quad A=\left(1+\frac{j\omega\Delta x^2}{2\alpha}\right) \tag{4}$$

$\alpha=k/\rho C$ is the sample thermal diffusivity.

The nodal equation for the rear face of the sample has been obtained by assuming it to be perfectly insulating. The nodal temperatures in these equations represent complex temperatures. Hence to obtain the temperature distribution in the sample a set of N complex linear equations need to be solved. An example of a typical matrix is given below for a sample divided into 5 nodal points.

$$\begin{bmatrix}-A & 1 & 0 & 0 & 0\\ 1 & -2A & 1 & 0 & 0\\ 0 & 1 & -2A & 1 & 0\\ 0 & 0 & 1 & -2A & 1\\ 0 & 0 & 0 & 1 & -A\end{bmatrix}\begin{bmatrix}T_1\\ T_2\\ T_3\\ T_4\\ T_5\end{bmatrix}=\begin{bmatrix}-\frac{Qdx}{k}\\ 0\\ 0\\ 0\\ 0\end{bmatrix} \tag{5}$$

The solution of these type of complex linear equations can be obtained by the use of commercial math software library. In the present case the computer software MathCad [9] and NAG [10] library routines were used. The former software package requires very little programming effort but is currently limited to solving a 30x30 complex matrix.

In computing a numerical solution using this technique care must be taken in the nodal spacing, Δx, used in the calculation. Solutions approaching the analytical values are obtained for $\Delta x \ll \mu$, where μ is the thermal diffusion length $\mu=\sqrt{2\alpha/\omega}$. This is demonstrated from the data presented in table 1. Table 1 compares the

Table 1. A comparison of the numerical and analytical solution for a semi-infinite medium with periodic surface heating.

	PHASE ANGLE (DEG.)			
Location	$\Delta x = 1\mu$	$\Delta x = 0.5\mu$	$\Delta x = 0.1\mu$	*ANALYTICAL VALUE*
$x = 0$	-58.302	-48.569	-45.141	-45.000
$x = \mu$	-110.045	-104.630	-102.413	-102.295
$x = 2\mu$	-161.565	-160.320	-159.557	-159.591

Table 2. The thermal wave phase difference between the analytical and numerical computation for a thin opaque coating on a thick substrate using a $\Delta x = 0.1\mu$.

	THERMAL THICKNESS L/μ				
	0.1	0.5	1.0	1.5	2.0
PHASE DIFFERENCE	-0.027	-0.132	-0.197	-0.205	-0.193

numerical and analytical solution with different Δx values for three locations in a semi-infinite sample with periodic surface heating. It is seen that with decreasing Δx spacing the numerical solution approaches that of the analytical. As a further test of this method, the thermal wave phase variation for a nickel chrome carbide coating on stainless steel was computed numerically at a frequency of 10 Hz. Table 2 shows the phase difference between the analytical and numerical calculations of this coating/ substrate system for different thermal thickness values, L/μ, and a $\Delta x = 0.1\mu$. The agreement between the numerical calculation and the analytical solution is very good.

The extension of this one dimensional treatment to two and three dimensions is straight forward. The only problems to be encountered will be the limit on array size to be solved. In these cases sparse matrix algorithms for solving complex linear equations will be required.

TRANSIENT TEMPERATURE DISTRIBUTIONS

Four finite difference techniques which are routinely used in transient heat conduction analysis are: a) explicit, b) fully implicit, c) implicit Crank-Nicolson (CN) and d) alternating direction implicit (ADI) methods. The explicit method yields directly the future temperature at a time step Δt, in terms of the current temperature. This numerical method is however subject to a stability criterion: $\alpha \Delta t / \Delta x^2 < 0.5$, which in some situation, may restrict the use of small grid size (Δx) and prove to be unsuitable if the calculations are to be performed over a long period of time. The fully implicit scheme offers no such restriction and the method is unconditionally stable for large time step. However, more computational work is required in solving a set of linear simultaneous equations for each time step.

CRANK-NICOLSON METHOD

The numerical schemes described above are only accurate to first order derivative approximations in space and time. The implicit CN method [7] utilises the advantages of the implicit scheme but also improves the numerical derivative approximations to second order accuracy in space and time. This is achieved by taking the arithmetic mean value of the spatial derivatives at the current and future time step. The finite difference form of the heat diffusion equation for one dimension is modified as:

$$\frac{1}{2}\left[\frac{T_{i+1}^{n+1}-2T_i^{n+1}+T_{i-1}^{n+1}}{\Delta x^2}+\frac{T_{i+1}^{n}-2T_i^{n}+T_{i-1}^{n}}{\Delta x^2}\right]=\frac{1}{\alpha}\left[\frac{T_i^{n+1}-T_i^{n}}{\Delta t}\right] \tag{6}$$

where i is the node position and superscripts n and n+1 refer to the temperature at the current and future time respectively. In applying the conservation of heat flux and continuity of temperature, similar difference equations can be deduced for the interface, surface and rear nodes if the boundary conditions of the sample are specified. These are listed in table 3 where it is assumed that surface heat flux is uniform in time and the rear face is insulated. The method of solution for N simultaneous nodal equations is similar to the example given in the periodic case with the coefficients of the unknown temperatures arranged in a tri-diagonal matrix which can be solved by Gaussian elimination.

Figure 1 illustrates the results computed for the logarithmic slope of the surface temperature transients of a step-pulse heating for various combination of layered materials. In our problem, much of the thermal transients cover a few decades in the logarithmic time scale. The computation process can be speeded up by splitting it up into several stages; each of increased time step and overlapped the previous one. Initial numerically induced oscillations can then be discarded. Although the CN technique is unconditionally stable, care must also be taken in the nodal spacing, Δx, in each layer if the solution is to be attained in a short time. The curves in Fig. 1 were computed using $5\Delta x < 2\sqrt{\alpha \Delta t}$ for four different time steps, each differed by an order of magnitude and each time step was performed over 200 calculations. The computation time for a 500 node points sample took approximately 5 minutes in compiled basic programming language on an IBM AT microcomputer.

Table 3. Nodal equations for the Crank-Nicolson finite difference expansions for the computation of transient thermal wave distribution.

Node position	**Finite Difference Expansion**
Surface Node 1	$(1+r)T_1^{n+1}-rT_2^{n+1}=(1-r)T_1^{n}+rT_2^{n}+\frac{2rQ\Delta x}{k}$
Interior Node i	$-rT_{i-1}^{n+1}+2(1+r)T_i^{n+1}-rT_{i+1}^{n+1}=r(T_{i-1}^{n}+T_{i+1}^{n})+2(1-r)T_i^{n}$
Interface Node s	$-r_1T_{s-1}^{n+1}+(D+r_1+r_2)T_s^{n+1}-r_2T_{s+1}^{n+1}=r_1T_{s-1}^{n}+r_2T_{s+1}^{n}+(D-r_1-r_2)T_s^{n}$
Rear Face Node M	$-rT_{M-1}^{n+1}+(1+r)T_M^{n+1}=r(T_{M-1}^{n}-T_M^{n})+T_M^{n}$
$D=(\rho_1C_1+\rho_2C_2)$	$r_i=\frac{2\alpha_i\Delta t}{\Delta x^2}$

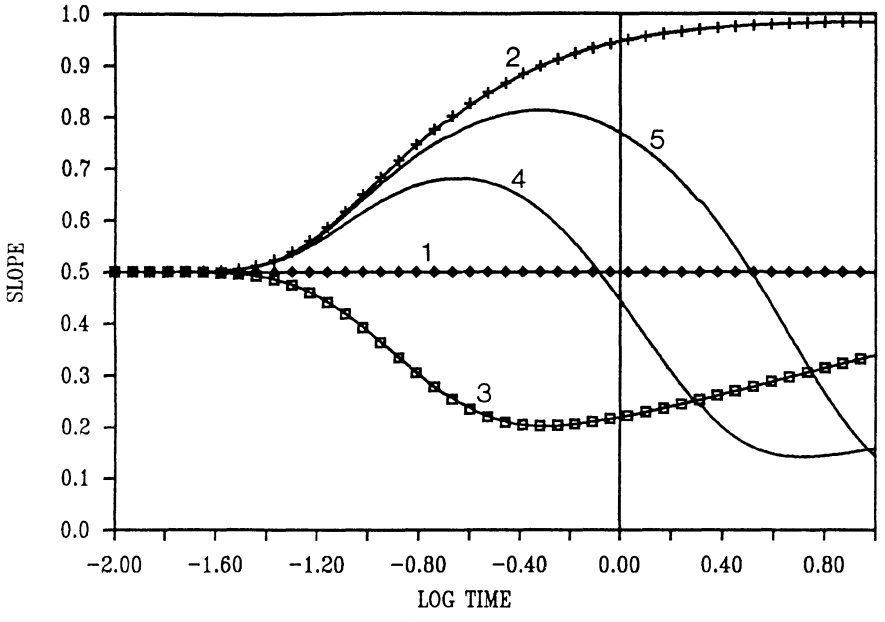

Figure 1. A one dimensional CN computation of the logarithmic slope of the surface temperature ((T/t).dT/dt) of a sample heated by a step heat pulse. Curves 1-3 compare the numerical results with the analytical solution obtained for a semi-infinite coating, 250μm zirconia film, and a 250μm zirconia coating on a steel substrate, respectively. Curves 4 and 5 are respectively, the numerical results for a 50 and a 100 μm air-gap defect sandwiched between a 250 μm zirconia coating and steel.

Curves 1, 2 and 3 show excellent agreement between numerical calculations and analytical solutions computed for homogeneous semi-infinite solid, zirconia coating with an air backing, and zirconia coating on stainless steel respectively. Curves 4 and 5 are the numerical predictions for an air-gap of 50μm and 100μm respectively, sandwiched in between a 250μm thick zirconia coating and a thick steel substrate.

ADI METHOD

In the ADI method the finite difference form of the two dimensional diffusion equation is decomposed into two separate equations as shown below for a homogeneous sample. These equations are alternately evaluated in each direction for half the time step. The energy balance method is again used to obtain the finite difference nodal equations.

Implicit x-direction:

$$r_x T^*_{i-1,j} - (2r_x + 1)T^*_{i,j} + r_x T^*_{i+1,j} = -r_y T^n_{i,j-1} + (2r_y - 1)T^n_{i,j} - r_y T^n_{i,j+1} \quad (7)$$

Implicit y-direction:

$$r_y T^{n+1}_{i,j-1} - (2r_y + 1)T^{n+1}_{i,j} + r_y T^{n+1}_{i,j+1} = -r_x T^*_{i-1,j} + (2r_x - 1)T^*_{i,j} - r_x T^*_{i+1,j} \quad (8)$$

where * denotes half time step and $r_x = \alpha\Delta t/\Delta x^2$, $r_y = \alpha\Delta t/\Delta y^2$. $T_{i,j}$ is the temperature at node position i,j. i= x coordinate and j= y coordinate.

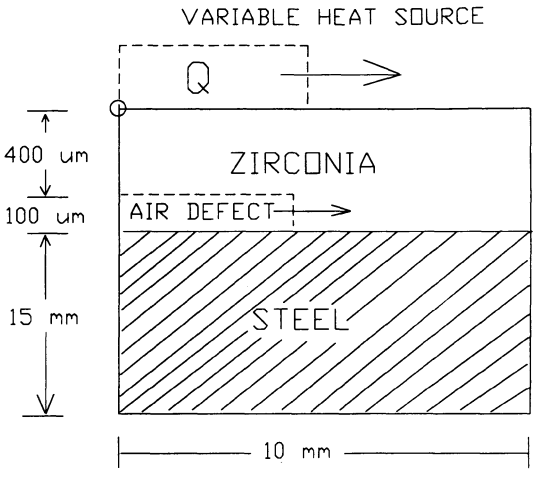

Figure 2 A schematic illustration of the test sample configuration modelled in Figs. 3 and 4 showing heat source and defect width variations.

In this scheme, only one of the spatial derivatives replaced by a central difference is implicitly evaluated at any time in terms of the unknown "future" nodal temperatures, while the central difference of the other spatial derivative is evaluated with the present known nodal temperatures. In each half time step the future temperatures are obtained by solving a tri-diagonal matrix. An application of the ADI method is presented below. The numerical computations were performed in Fortran on an IBM AT microcomputer. The calculations took 40 minutes to evaluate 200 time steps for a grid spacing of 100 by 100 nodes.

Consider a sample of 400μm thick zirconia coating on steel substrate with the inclusion of a 100μm air gap at the interface in two dimensions, see Fig. 2. A heat source such as a laser or heat gun is constantly applied to the sample surface and an infrared detector is focused onto the center spot to monitor its surface temperature transients. Because of symmetry only one half of the geometry is necessary and that the exposed boundaries are insulated. The numerical computations for the logarithmic slope of the thermal transients are performed using two different time step sizes differing by an order of magnitude, each covering 100 time step calculations. The results are shown in Fig. 3 for a plane heat source and in Fig. 4 for a line heat source. Because of symmetry, curves 1 and 4 of Fig. 3 are checked in good agreement with the one dimensional analytical solution for a 2-layer system and with the CN numerical solution.

The affect of defect width on the surface transients are shown by curves 2 and 3 (Fig.3). At short time the sample behaves like a semi-infinite medium with an initial slope of half. With increasing time the departure from this slope of a half is due to thermal wave interference effects which occur when the transient thermal diffusion length, $\mu_t = 2\sqrt{\alpha t}$, approaches that of the defect depth. The direction of change of the slope depends on the thermal impedance mismatch between zirconia, air-defect and steel. The reduction in slope magnitude with decreased defect width results from the thermal wave interference contributions of reduced constructive components from the defect region and the increased destructive components from the zirconia-steel interface.

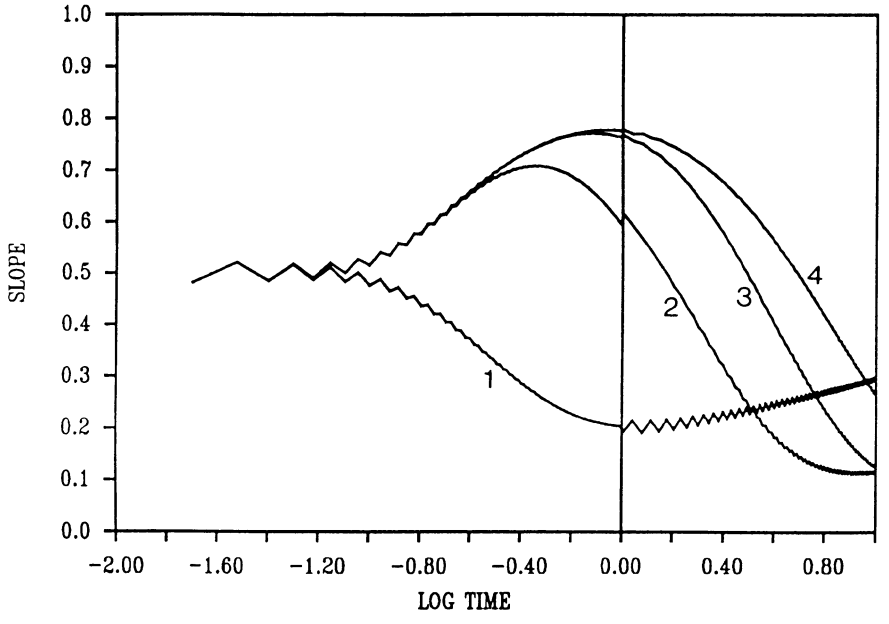

Figure 3 Variation of the slope of the surface temperature with time computed at the position O for plane surface heating of the sample shown in Fig. 2. Curve 1) no defect, 2) 1 mm, 3) 2 mm and 4) 10 mm half width defect.

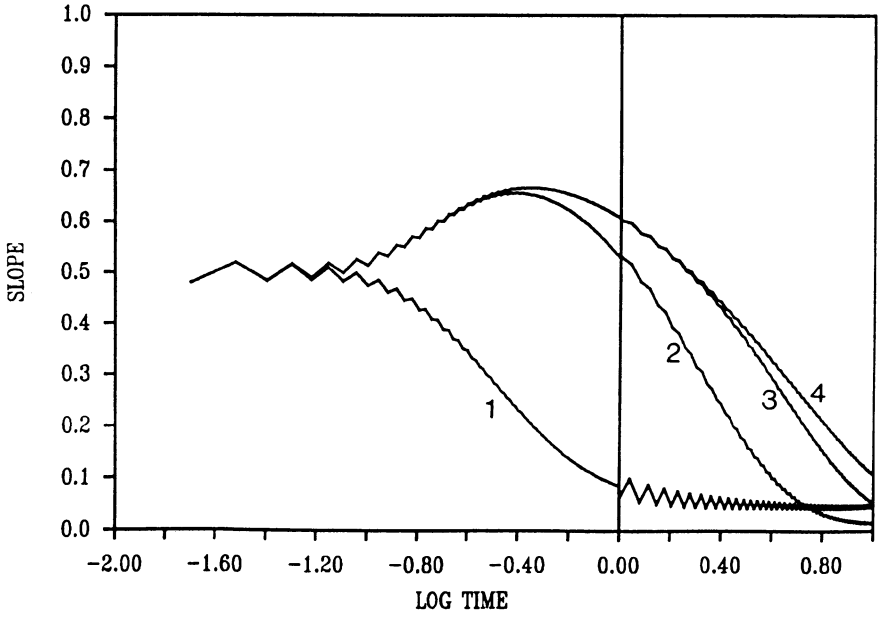

Figure 4 Variation of the slope of the surface temperature with time computed at the position O for a localised heat source of half width 1 mm of the sample discussed in Fig. 3.

Figure 4 shows the slope versus log. time curves for the above discussed samples using a line heat source of half width R=1 mm. With this localised heat source, heat can diffuse in two directions one normal and the other parallel to the sample surface. In comparing Figs. 3 and 4, it is seen that there is a reduction in the overall slope magnitude in all cases and slope contrast between different defect widths with the localised heat source. This results entirely from the change in the balance of the relative contributions of the thermal reflections from the defect and the coating/ substrate interface. From this numerical example it appears that in the detection of finite size defects, plane heating is preferable over localised heating.

SUMMARY

Finite difference methods of heat conduction analysis have been applied to compute periodic and transient surface temperatures. It is shown that to obtain accurate values of the complex surface temperature, for the periodic heating case, the condition $\Delta x \ll \mu$ must be satisfied. For transient heating case a similar condition also applies. In the CN case $\Delta x \ll \mu_e$ is required. With the ADI method the same spacing criterion also applies in both directions, but it is less restrictive if the temperature gradient in one direction is not sharp.

ACKNOWLEDGEMENTS

The authors would like to acknowledge the financial support of the Science and Engineering Research Council and Central Electricity Generating Board for their support for this research.

REFERENCES

1 Physical Acoustics 18; Ed W.P Mason and Thruston. (Academic Press, New York, 1989)
2 Review of Progress in Quantitative NDE. 8A and 8B; ed., D.P Thompson and D.E. Chimenti, (Plenum Press, 1989)
3 Photothermal Investigations in Solid and Fluids. ed., J.A. Sell, (Academic Press, New YorK, 1989)
4 Photoacoustics and thermal wave phenomena in semiconductors. ed., A. Mandelis, (North Holland Press, 1987)
5 Y. Jaluria and K.E. Torrance, Computational Heat Transfer. (Hemisphere Pub. Company, 1986)
6 O.C. Zienkiewicz, The Finite Element Method, 3rd Edition. (McGraw-Hill, 1986)
7 Boundary Element Methods. X. ed.,C.A. Brebbia, (Comput. Mech. Pub, 1988)
8 K.J. Baumeister, Heat Transfer: Research and application, AIChE Symp. Ser. 74(174) p243-249 (1978)
9 Mathsoft Int. One Kendall Sq., Cambridge, MA 02139, USA.
10 NAG Ltd, Wilkinson House, Jorden Hill Road, Oxford, OX2 8DR. England